Hong, Gonghua; Cheng, Haitao; Zhang, Shuanbao; Rojas, Orlando J.

Mussel-inspired reinforcement of a biodegradable aliphatic polyester with bamboo fibers

Published in:
Journal of Cleaner Production

DOI:
10.1016/j.jclepro.2021.126587

Published: 10/05/2021

Document Version
Publisher's PDF, also known as Version of record

Journal of Cleaner Production 296 (2021) 126587

Contents lists available at ScienceDirect

Journal of Cleaner Production

journal homepage: www.elsevier.com/locate/jclepro

Mussel-inspired reinforcement of a biodegradable aliphatic polyester with bamboo fibers

Gonghua Hong [a, b, c], Haitao Cheng [e], Shuangbao Zhang [a, b, **], Orlando J. Rojas [c, d, *]

[a] Beijing Key Laboratory of Wood Science and Engineering, Beijing Forestry University, Beijing 100083, China
[b] MOE Key Laboratory of Wooden Material Science and Application, Beijing Forestry University, Beijing 100083, China
[c] Department of Bioproducts and Biosystems, Aalto University, Vuorimiehentie 1, Espoo, P.O. Box 16300, FI-00076, Aalto, Finland
[d] Bioproducts Institute, Departments of Chemical & Biological Engineering, Chemistry, and Wood Science, The University of British Columbia, 2360 East Mall, Vancouver, BC V6T, 1Z3, Canada
[e] Bamboo and Rattan Science and Technology Key Laboratory of the State Forestry Administration, International Centre for Bamboo and Rattan, Beijing, 100102, PR China

ARTICLE INFO

Article history:
Received 9 November 2020
Received in revised form
13 February 2021
Accepted 1 March 2021
Available online 2 March 2021

Handling editor: Cecilia Maria Villas Bôas de Almeida

Keywords:
Bamboo fiber
PBS-Based biocomposites
Polydopamine
Interfacial adhesion

ABSTRACT

Natural fiber-reinforced biocomposites displaying light weight, low thermal conductivity and reduced environmental footprint are increasingly relevant in structural, packaging, cementitious and masonry materials. However, the poor interfacial compatibility between fibers and typical polymers has limited the development of mechanical strength and water resistance. Here, we report a green, facile and effective method inspired by nature to promote interfacial adhesion in biocomposites based on a biodegradable aliphatic polyester (polybutylene succinate, PBS). For this purpose, PBS was reinforced with bamboo fibers modified with (3-aminopropyl) triethoxysilane and polydopamine (PDA). The PDA deposition and covalent adhesion with the fibers were promoted by self-polymerization and Michael addition and/or Schiff based secondary reactions. A distinct improvement in reinforcement was achieved together with gains in performance, including tensile strength (70%), tensile modulus (25%), flexural strength (37%), flexural modulus (24%) and impact strength (63%). The results far exceeded those measured for other fiber-reinforced biocomposites while simultaneously introduced water resistance.

1. Introduction

The expanding environmental pollution and need for energy have stimulated the adoption of eco-friendly materials as an alternative to petrochemical-based plastics and related products (Khalil et al., 2012). In this regard, bio-based polymers derived from natural resources have been frontrunners for their intrinsic renewability and biodegradability (Iwata, 2015). Among others, polybutylene succinate (PBS) is a promising bio-based polymer that can be synthesized from bio-refined succinic acid (or dimethyl succinate) and 1,4-butanediol. PBS has attracted increased attraction for its thermal properties (Gigli et al., 2016; Lee et al., 2005). However, limited mechanical properties and cost are major barriers preventing the adoption of PBS in large-scale applications (Huang et al., 2018).

Natural fibers are noteworthy for their abundance, low density, biodegradability and eco-friendliness, and have emerged as preferred options to reinforce bio-based polymer composites (Faruk et al., 2014; Majeed et al., 2013). Natural fiber-reinforced biocomposites can be produced to achieve a low thermal conductivity and density and to find uses in a number of applications (Akubueze et al., 2019; Claramunt et al., 2016; Dahy, 2019; Fazita et al., 2016; Ferreira et al., 2018; Gopinath et al., 2019). Among the various natural fibers, those derived from bamboo are distinctive for their small microfibrillar angle (~10°) and superior mechanical strength as well for their easy access from fast growing

* Corresponding author. Department of Bioproducts and Biosystems, Aalto University, Vuorimiehentie 1, Espoo, P.O. Box 16300, FI-00076, Aalto, Finland.
** Corresponding author. Beijing Key Laboratory of Wood Science and Engineering, Beijing Forestry University, Beijing, 100083, China.
E-mail addresses: shuangbaozhang@163.com (S. Zhang), orlando.rojas@ubc.ca (O.J. Rojas).

https://doi.org/10.1016/j.jclepro.2021.126587

bamboo plants. Thus, they are promising candidates in natural fiber-reinforced biocomposites (Liu et al., 2012; Tang et al., 2015; Xu et al., 2010a). Nevertheless, similar to other lignocellulose fibers, the inherent hydrophilicity of bamboo fibers presents a challenge as far as compatibility, aggregation and water sorption, preventing a more widespread use (Dahy, 2019; Vaisanen et al., 2017).

Responding to such drawbacks, several strategies have been applied, such as fiber treatments (including alkali and heat treatment, steam explosion and esterification modification) and chemical coupling (silane and maleic anhydride–grafted copolymers) (Gao et al., 2016; Perez-Fonseca et al., 2015; Takatani et al., 2000; Wei et al., 2013; Xu et al., 2010b; Zhang et al., 2015). This has opened new opportunities in clothing, biomedical and pharmaceutical materials, sports, aerospace and electromagnetic applications (Kohan et al., 2019; Scarponi and Messano, 2015; Tavares et al., 2020; Xia et al., 2017; Yusup et al., 2019). However, owing to the reaction conditions, the surface modifications used to improve the compatibility between the lignocellulose fibers and the polymer matrix usually entail a reduction in strength. This factor, together with the added capital costs and the release of toxic gases, prevent or limit a wide adoption by industry. Therefore, there is a pressing need to achieve clean, effective, and sustainable surface modifications that are easy to implement toward superior performance.

A possibility to reinforcing interfaces can be drawn from the ability of mussel byssus as adhesive. Its superior performance is produced by secreted proteins and the effect of 3,4-dihydroxyphenylalanine and lysine amino acids that are high chemically reactive and facilitate strong interfacial interactions. Moreover, substrates of organic or inorganic origins can be modified using simple reaction conditions (Xiong et al., 2014). Inspired by the adhesive proteins, dopamine, a small catechol molecule containing terminal amino groups, has been used to oxidatively self-polymerize in mild alkaline pH, similar to the typical marine environment that leads to the formation of adhesive polydopamine (PDA) (Lee et al., 2007; Levy et al., 2003; Zhang et al., 2014). PDA functional coatings are some of the simplest and the most powerful alternatives available for surface modification and to achieving engineered materials in combination with nanoparticles, nanotubes, nanowires, microbeads, organic or inorganic components (Gao et al., 2018; Huo et al., 2019; Meng et al., 2017; Palladino et al., 2019; Song et al., 2018; Wu et al., 2017b, 2018; bF.C. Wu et al., 2017; Zhao et al., 2018). Furthermore, catechol in PDA coatings is capable of anchoring various functional groups for secondary reactions through covalent or noncovalent binding interactions (Lee et al., 2011; Lu et al., 2015; Tang et al., 2019). Mussel-inspired adhesives offer a versatile surface chemistry to develop composites with biological, chemical, energy, and environmental features (Palanisamy et al., 2016; Peng et al., 2017; Shukla et al., 2018; Wang et al., 2017; W.H. Wu et al., 2017).

In this work, amino silane grafting was selected to work synergistically with secondary reactions in PDA- functionalized bamboo fibers. The abundant active sites (−NH_2/−OH groups) of the PDA coating on the bamboo fiber created a versatile platform for reaction with the hydrolyzed amino silanol generated from (3-aminopropyl) triethoxysilane (APTES), with the secondary grafting of amino silane realized through Michael addition and/or Schiff base reactions (Hao et al., 2016; Hwang et al., 2014; Lee et al., 2016). The hybrid coating on the bamboo fiber surface was confirmed by SEM, FT-IR, XPS and XRD. The effect of the modified bamboo fibers on the mechanical properties, water resistance, hygroscopicity and interfacial interactions of the reinforced PBS-based biocomposites were investigated. The results indicate the successful synthesis of high-performance, eco-friendly PBS-based biocompositesfollowing mussel-inspired adhesives.

2. Materials and methods

2.1. Materials

Bamboo fibers were reduced in size by using a mechanical crusher (uluS5C, GREAT, China) (40–60 mesh, fiber length < 380 μm) and supplied by Anhui Sentai WPC New Material Co. Ltd. (Anhui, China). Polybutylene succinate (PBS) (density = 1.24 g/cm^3, flow index = 2.0 g/10 min and crystallinity = 32%) was purchased from Anqing Hexing Chemical Co., Ltd. (Anhui, China). Dopamine hydrochloride (DA) (assay ≥98.5%), tris(hydroxymethyl aminomethane) (tris) and (3-aminopropyl) triethoxysilane (APTES, KH550, 99%) were purchased from Duly Biotech Co., Ltd. (Nanjing, China). Other reagents, including deionized water, anhydrous ethanol, and paraffin wax, were analytical grade and purchased from Beijing Chemical Works, China.

2.2. Surface modification of bamboo fibers with PDA and APTES

The bamboo fibers were firstly washed repeatedly with deionized water and anhydrous ethanol to remove the impurities on the surfaces, after drying at 80 ± 2 °C for 24 h, the obtained fibers were denoted as BF. Surface modification with PDA was carried out by adding 5 g BF and 2.0 mg/mL dopamine in 100 mL tris buffer solution (pH 8.5). The suspension was subsequently stirred at room temperature for 24 h; after washing and drying, the resulting product was denoted as "PDA-BF". Amino silane secondary grafting was then produced by adding 5 g BF and 2.0 mg/mL dopamine into 100 mL tris buffer solution (pH 8.5), stirred at room temperature for 24 h and followed by dropwise addition of APTES at five different concentrations (0.1, 0.2, 0.4, 0.6, and 0.8 mg/mL). APTES-grafted bamboo fibers (K–BF) were obtained by adding 5 g BF and 0.6 mg/mL APTES in 100 g hydrous ethanol solution and stirring at room temperature for 24 h. More information about the experimental procedures can be found in Note S1 of the Supporting Information. The experimental details and material composition is summarized in Table 1 and the modification process is illustrated in Fig. 1.

2.3. Preparation of fiber-reinforced PBS biocomposites

The bamboo fiber-reinforced PBS biocomposites were fabricated using a process that included mixing, extrusion and hot-pressing. More details of the preparation process can be found in **Note S2**. The labels used herein for the various PBS-based biocomposites followed the nomenclature of the corresponding bamboo fibers, see Table 1. The details of the preparation process and proposed reactions and mechanism of fiber-reinforced PBS biocomposites are illustrated in Fig. 1.

Table 1
Experimental details for bamboo fiber surface modification (BF refers to bamboo fibers, unmodified or modified with P= polydopamine (PDA) and/or K=(3-aminopropyl) triethoxysilane).

Sample	Bamboo fiber (g)	Dopamine (mg/ml)	APTES (mg/ml)
BF	5	–	–
PDA-BF	5	2	–
K–BF	5	–	0.6
P/K–BF-1	5	2	0.1
P/K–BF-2	5	2	0.2
P/K–BF-3	5	2	0.4
P/K–BF-4	5	2	0.6
P/K–BF-5	5	2	0.8

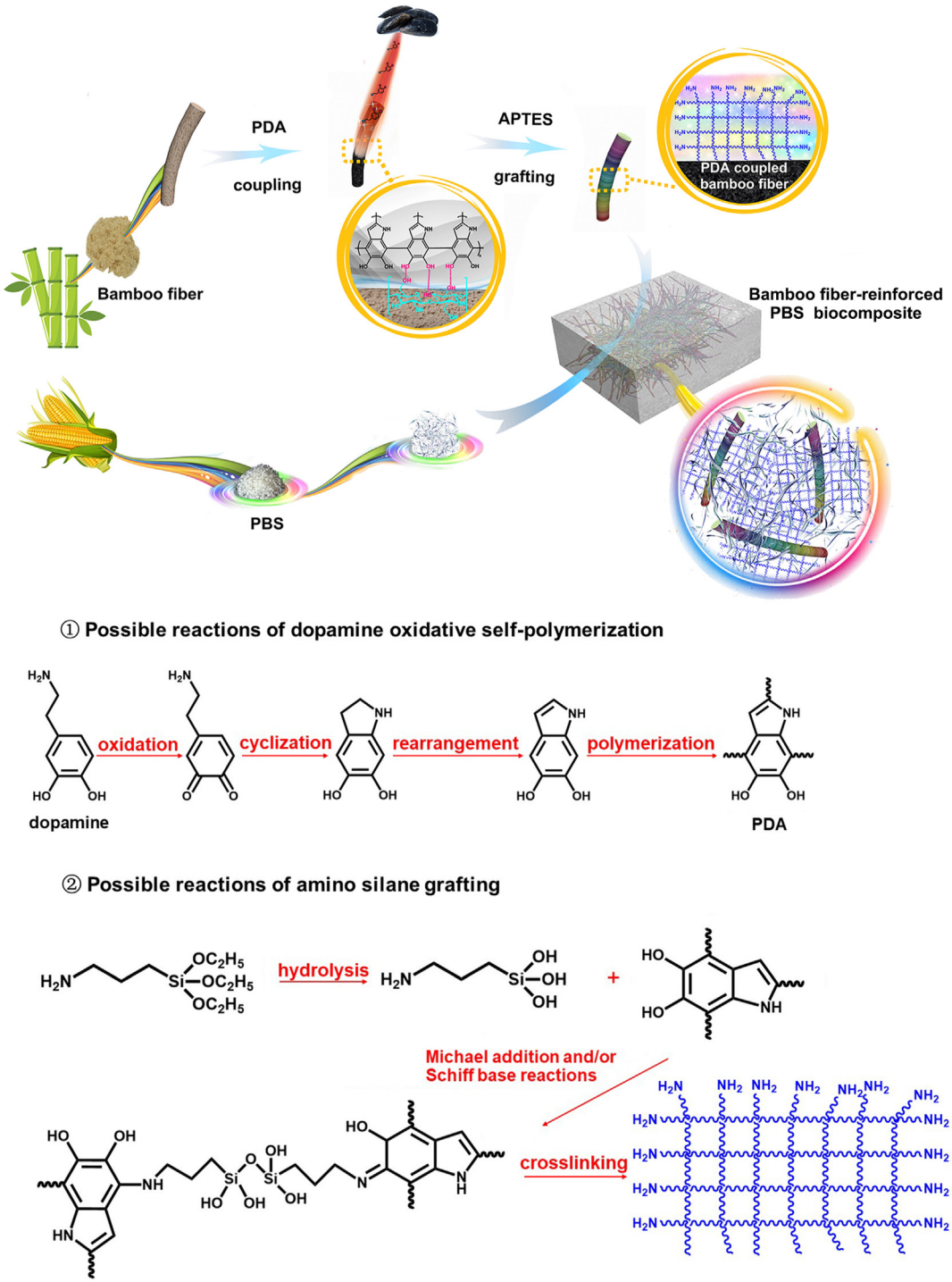

Fig. 1. Schematic illustration of the modification of bamboo fibers and preparation of PBS-based biocomposite.

2.4. Characterization

The surface morphology and structural features of bamboo fibers were investigated with field emission scanning electron microscopy (FE-SEM, Hitachi SU8010) operated at an accelerating voltage of 10 kV. Before observation, all samples were coated with gold to prevent electron beam charging.

The chemical changes in bamboo fibers were investigated using Fourier transform infrared spectroscopy (FTIR, Vertex 70v, Bruker, Karlsruhe, Germany) using a wavelength range of 500–4000 cm^{-1}. The surface chemical/elemental states of the bamboo fiber were examined by X-ray photoelectron spectroscopy (XPS, ESCALAB250) using Al Kα radiation source ($h\nu = 1486.7$ eV).

The crystallization behavior of the bamboo fibers was investigated by X-ray diffraction (XRD, Bruker D8) with a Cu Ka ($\lambda = 1.542$ Å) radiation source. The experiments were conducted at 40 kV and 40 mA, with a theta scan ranging from 0° to 40° at 5 min/° intervals. The relative crystallization index was calculated following Equation (1).

$$\textit{Relative Cristallinity Index}\ (\%) = \frac{I_{002} - I_{am}}{I_{am}} \times 100\% \quad (1)$$

where I_{002} is the peak strength of the 002 crystalline plane, and I_{am} correspond to the intensity of the non-crystalline plane.

The tensile and flexural properties of the PBS-based biocomposites were measured using a universal testing machine (Kexin Instrument Equipment Co. Ltd., Changchun, China). The impact property of PBS-based biocomposites was measured by a cantilever beam impact tester (Hebe Precision Testing Machine Co. Ltd., Chengde, China). More details of the measurements of the mechanical properties of biocomposites can be found in **Note S3**. Six replicates were used in the measurements of tensile, flexural and impact properties, the average values were calculated to reflect the final results. To understand the possible interactions present in the composites, we conducted molecular dynamics simulation (Forcite Module under the COMPASS force field).

The dynamic mechanical analyses of the PBS-based biocomposites were conducted by Dynamic Thermomechanical Analyzer (DMA, NETZSCH, Selb, Germany) using samples with dimensions of 35 × 10 × 4 mm^3. The measurements were conducted at a temperature ranging from −60 to 40 °C (heating rate of 3 °C/min), under a single cantilever bending mode at a scanning frequency of 1 Hz.

The fracture surface morphology and structure of PBS-based biocomposites were examined with a field emission scanning electron microscopy (FE-SEM, Hitachi SU8010) at an accelerating voltage of 10 kV. Before observation, all samples were coated with gold adequately to prevent electron beam charging.

The hygroscopicity of the PBS-based biocomposites was examined via a Dynamic Vapor Sorption (DVS) measurements (ANALYX CORP, America) under a relative humidity (RH) varying from 5% to 95% using 10% RH intervals. The measurements were conducted in dry nitrogen (N_2) atmosphere at 25 °C.

The water resistance of the PBS-based biocomposites was evaluated based on the ASTM D5229-12 standard. Before measurement, all samples (50 mm × 50 mm × 4 mm) were dried at 80 ± 2 °C until reaching constant weight. The dried samples were subsequently dipped in distilled water at 25 ± 1 °C for 13 days and weighed at intervals of 12 h. The experiment was performed at 40–50% RH. Each group consisted of six samples and the resultant % water absorption was determined using Equation (2).

$$\text{Water absorption}(\%) = \frac{(W_t - W_d)}{W_d} \times 100\% \quad (2)$$

where W_d and W_t represent the average values of the weight of dried sample, and the weight at the given intervals, respectively.

3. Results and discussion

3.1. Morphology of bamboo fibers

Unmodified bamboo fibers showed comparatively smooth surfaces (Fig. 2a), while a thin and rough PDA coating was clearly observed upon surface modification with PDA (Fig. 2b). Following APTES grafting, small crystals and particles were generated on the surfaces of the rougher bamboo fibers (Fig. 2c), indicating the generation of a hybrid PDA-silanol coating. The possible, respective reactions are presented in Fig. 1. We speculate that PDA was coupled with the surface of the bamboo fiber. Meanwhile, free PDA was spontaneously bound with the hydrolyzed APTES via Michael addition and/or Schiff-based reactions under alkaline conditions. This resulted in the formation of crosslinked PDA-silanol network on the bamboo fiber surface (Lee et al., 2007). An apparent increase in surface roughness was observed with the addition of APTES (Fig. 2d, e and 2f). Excess APTES did not increase the reaction sites of PDA-coated bamboo fibers; instead, it caused self-reactions that led to aggregated silanol crystals around fibers, as shown in Fig. 2f and g. In the absence of PDA, only a small amount of APTES was physically adsorbed on the fibers (Xie et al., 2010), with the appearance of self-reacted silanol crystals (seen in Fig. 2h). Overall, the SEM observations indicate the significant role of PDA coating to increase surface activity and reactive sites on the bamboo fibers.

3.2. Chemical changes

For bamboo fibers, the IR absorption peaks were located at ca. 3435 cm^{-1}, assigned to −OH stretching vibrations, and 2900 cm^{-1}, assigned to C−H stretching vibrations (Gu et al., 2013; Tang et al., 2015). After modification with APTES, a slightly enhanced intensity in the fingerprint region located near 1070 cm^{-1} and 1130 cm^{-1} in K−BF curve was observed, assigned to the Si−O−C/Si−O−Si and Si−O stretching vibrations. The results suggest successful introduction of hydrolyzed amino silanol (Fang et al., 2014). Compared with the unmodified bamboo fibers, the two enhanced absorption peaks around 2900 cm^{-1} in PDA-treated bamboo fiber corresponded to $-CH_3$ and $-CH_2-$ stretching vibrations generated by PDA molecules, respectively (Chen et al., 2017), which proved the successful reaction of PDA on the surface of the fibers. Lignin and polyphenolic extracts possess similar functional groups as those of PDA, obscuring a clear elucidation of the changes, which were further investigated by XPS. Additional experiments based on molecular dynamics simulation (Forcite Module under the COMPASS force field) were carried out to clarify the formation of hydrogen bonding between the PDA molecule and bamboo fibers (**Note** S4 and Figure S3). After amino silane grafting, two clear characteristic peaks ($-CH_3$ and $-CH_2$) were observed. Moreover, new peaks in the fingerprint region at around 1630, 1130 and 1070 cm^{-1} were observed, assigned to C=N, Si−O and Si−O−C/Si−O−Si stretching vibrations, respectively (Salarizadeh et al., 2016; Yuan et al., 2017; Zhan et al., 2018). They indicated the successful formation of crosslinked PDA-silanol network on the bamboo fiber surface. The four peaks near 1742, 1420, 1370 and 1165 cm^{-1} corresponded to C=O, $-CH_2-$, C−H and C−O−C vibrations, respectively, which were assigned to cellulose, hemicellulose and lignin in unmodified bamboo fibers (Zhang et al., 2015). The positions of these four characteristic peaks remained fairly unchanged after the introduction of PDA or PDA-silanol treatments (Fig. 3).

3.3. Surface chemical composition

The characteristic elements of all samples, determined by XPS, mainly included C1s and O1s (Liu et al., 2016). A new N1s peak was observed in the spectra obtained for PDA-BF and P/K−BF-4, attributed to surface coupling with PDA (Fig. 4a). The C1s high resolution spectrum of PDA−BF was curve-fitted for the five characteristic binding energies (BE) of 283.6 eV for C−C and C−H species, 285.8 eV for C−O, 286.8 eV for C=O and O−C−O, and 288.1 eV for O−C=O (Fig. 4b and Table S1) (Xu et al., 2013). As expected, an additional peak appeared in the C1s high resolution spectra of PDA−BF, near 285.5 eV for C−N, suggesting the successful introduction of PDA on the fiber surface. The N1s high resolution spectra of PDA−BF was fitted to peaks with binding energies of 401.7 eV for R_1-NH_2, 399.6 eV for R_1-NH-R_2 and 398.3 eV for C=NR (Feng et al., 2016) (Fig. 4c and Table S2). After amino silane grafting onto the PDA-treated fibers, the concentration of R_1-NH-R_2 (secondary amine) and C=NR (tertiary or aromatic amine) species

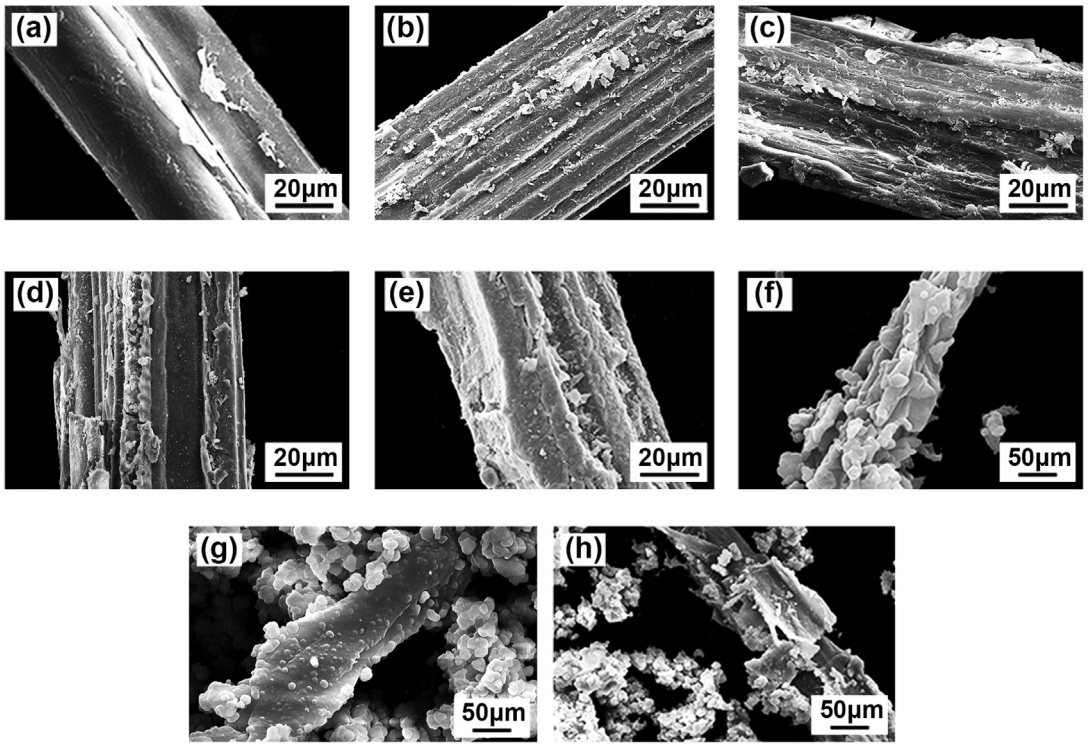

Fig. 2. SEM images of **(a)** BF; **(b)** PDA-BF; **(c)** P/K–BF-1; **(d)** P/K–BF-2; **(e)** P/K–BF-3; **(f)** P/K–BF-4; **(g)** P/K–BF-5; and **(h)** K–BF.

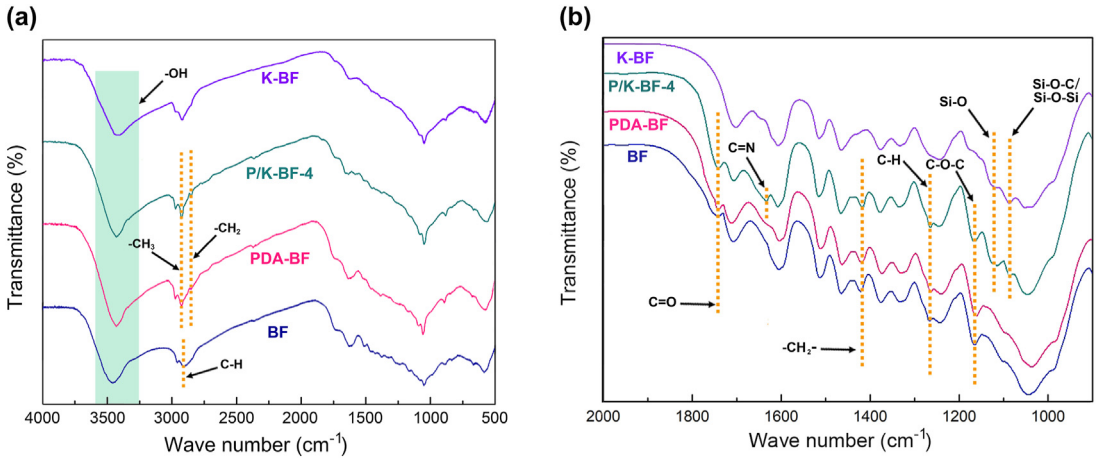

Fig. 3. **(a)** The FTIR spectra of the BF, PDA-BF, P/K–BF-4 and K–BF; and **(b)** the fingerprint region spectra from 2000 cm^{-1} to 900 cm^{-1} of the BF, PDA-BF, P/K–BF-4 and K–BF.

increased from 82.7% to 85.6% and from 3.5% to 7.8%, respectively, accounting for the grafting of amino silanol on the PDA-treated fibers via Michael addition and/or Schiff-base reactions (Fig. 4d and Table S3), as illustrated in Fig. 1. Also, a new Si2p peak was observed in the wide spectrum scan of PDA/K–BF-4. The changes demonstrated the successful secondary grafting of amino silane onto the PDA-coated bamboo fibers. Combined with the FTIR spectra, the results confirm the successful introduction of PDA and PDA-silanol on the surface of the bamboo fibers.

3.4. Bamboo fibers crystallinity

For unmodified bamboo fibers, the XRD peaks at 2θ of 17°, 22.5° and 35° were assigned to (101), (002), and (040) planes, respectively, fitting the characteristic diffraction peaks typical of the cellulose I crystal structure (Yao et al., 2017). Upon grafting amino silane, no distinct changes in peak position or shape were observed in the XRD profiles, suggesting negligible changes in the crystallinity of amino silane-grafted fibers. These results are partly ascribed to the formation of intermolecular hydrogen bonds in the hydrolyzed silane and fiber interfaces, which did not produce any significant effect on the crystal structure of the fibers (Chen et al., 2012). Upon introduction of PDA and PDA-silanol treatments, no changes were observed in the characteristic diffraction peaks, diffraction profiles and 2θ angles compared to those unmodified counterparts (Fig. 5).

3.5. Mechanical properties of the biocomposites

The static mechanical properties of the biocomposites, including

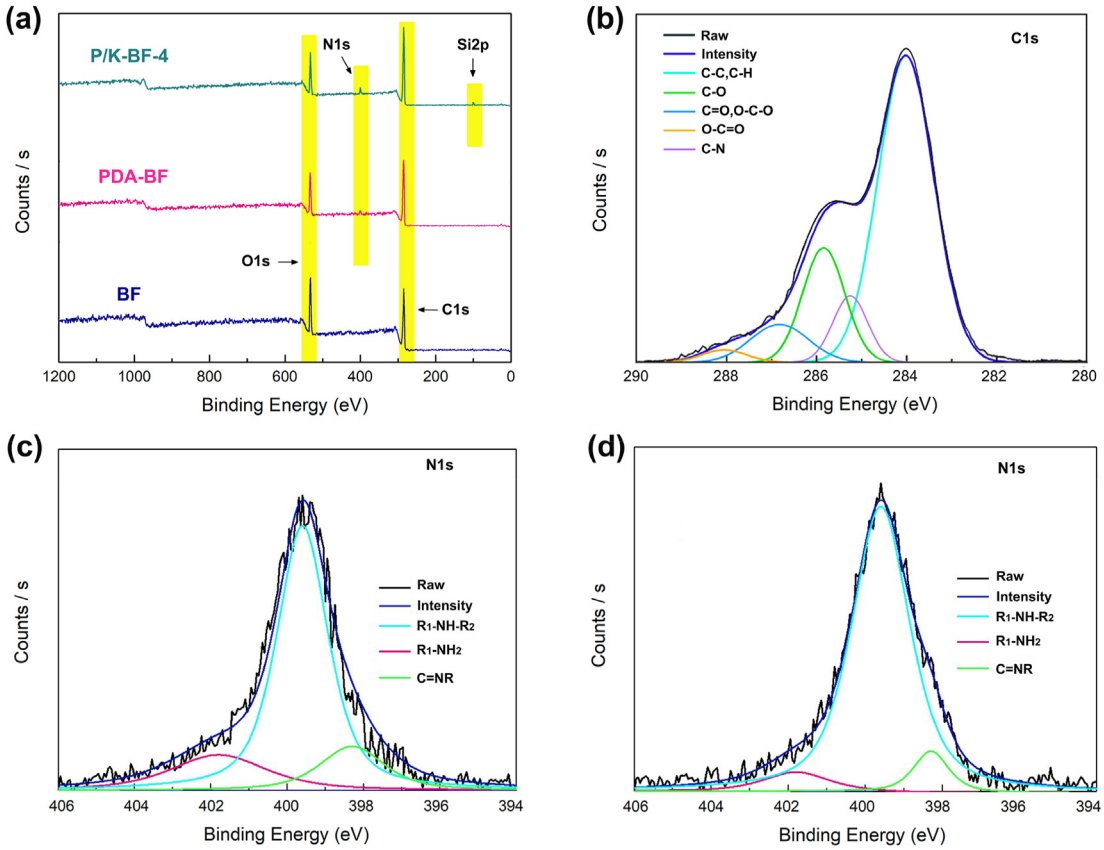

Fig. 4. XPS wide-scan and high-resolution spectra of bamboo fiber samples: **(a)** wide-scan XPS spectra of the BF, PDA-BF and P/K–BF-4, **(b)** C1s of PDA–BF; **(c)** N1s of PDA–BF; and **(d)** C 1s of P/K–BF-4.

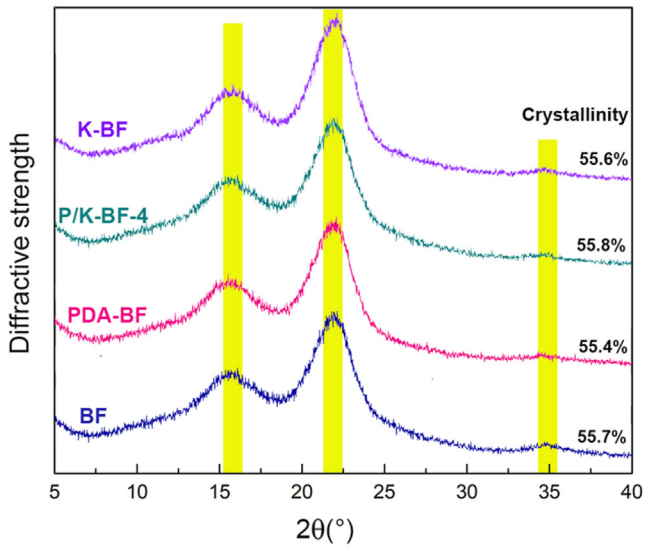

Fig. 5. XRD patterns of BF, PDA-BF, PDA/K–BF-4 and K–BF.

tensile, flexural and impact properties are crucial to evaluate the effects of interfacial interactions, as shown in Fig. 6. The tensile and flexural properties of PBS-based biocomposites containing K–BF were enhanced compared with those that were reinforced with the unmodified fibers. This is rationalized by the effect silane coupling on the surface of the bamboo fiber and with the PBS matrix, promoting stress transfer and supporting loading without structural damage (Yang et al., 2020). All the static mechanical properties increased with the introduction of PDA, owing to the PDA molecular interactions with the PBS chains (benzene ring and C–H chains), leading to an improved interfacial interaction. The greater improvement in the static mechanical properties of the PBS-based biocomposites was observed after the amino silane secondary grafting. The best static mechanical properties were observed for P/K–BF-3: compared to biocomposites reinforced with unmodified bamboo fibers, the tensile strength, tensile modulus, flexural strength, flexural modulus, and impact strength were improved by 70, 25, 37, 24 and 63%, respectively. Importantly, the tensile strength of the P/K–BF-3 composite was compared with that reported for other natural fiber-reinforced polymer composites (Table S4). It was found that the improvement in tensile strength surpassed most of the reported fiber/polymer composites. The results indicate the establishment of a network covalently attached to the surface of the bamboo fiber, via the effect of PDA and amino silane molecules, which interacted with PBS and restricted the chain mobility under external load. In addition, the increased surface roughness, given by PDA-silanol network, may have enhanced the interfacial interlocking between the fibers and the PBS matrix, which generated a tougher interfacial adhesion. As a consequence, the static mechanical strength was improved. When used in excess, the APTES self-reaction, generated aggregated crystals, which impaired the interfacial interaction between the fibers and the PBS matrix. This caused a negative effect on the static mechanical properties of PBS-based biocomposites, especially the impact strength.

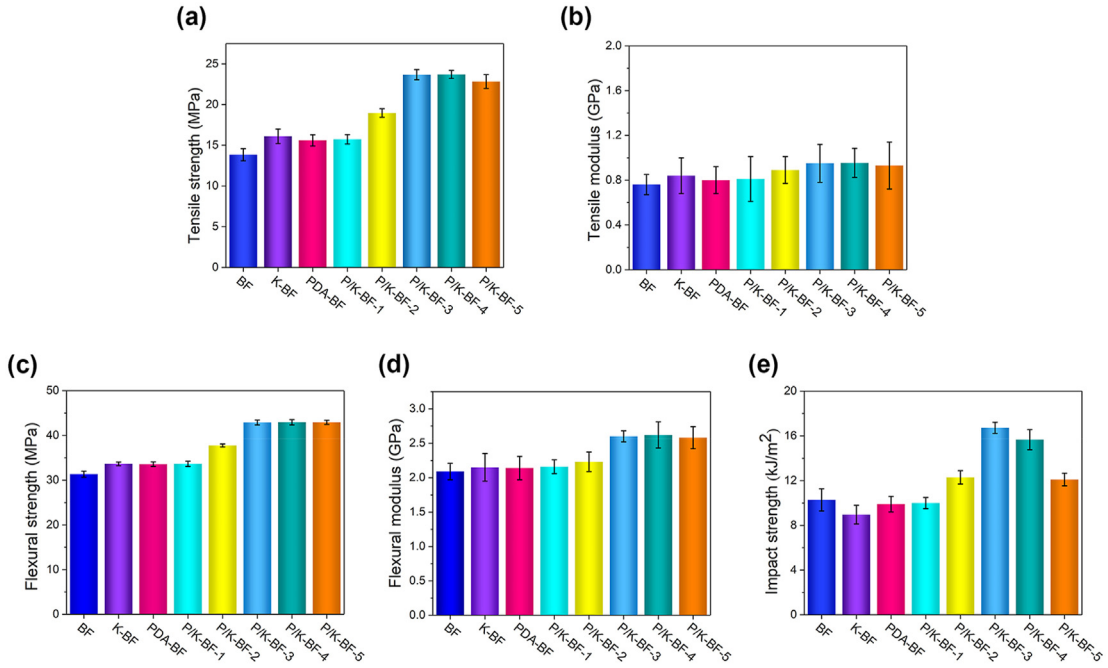

Fig. 6. Static mechanical properties of PBS-based biocomposites: **(a)** tensile strength; **(b)** tensile modulus; **(c)** flexural strength; **(d)** flexural modulus; and **(e)** impact strength.

3.6. Dynamic mechanical analysis

The storage modulus, the loss modulus and the (tan delta) factor were determined by oscillatory dynamic loading under increased temperature, taken as important indicators to estimate the interfacial adhesion in the materials. Owing to the PBS matrix, the biocomposites showed a reduced storage modulus with the increased temperature, from −60 to 40 °C (Fig. 7a), which is typical of the thermoplastic characteristics of PBS (Chen et al., 2017). The introduction of PDA and APTES enhanced the interfacial interaction of the as-prepared PBS-based biocomposites, which induced an increased storage modulus. In addition, the toughness of rigid PDA nanoparticles and silanol crystal might have also been a factor explaining the changes in the storage modulus (Zhou et al., 2014). A better interfacial behavior was achieved with the secondary grafting (amino silane onto the PDA-treated fibers), which resulted in an increased storage modulus. Moreover, with a moderate increase of APTES addition, the interfacial adhesion and stress transfer between the bamboo fiber and PBS was further improved, achieving an higher storage modulus. As a result, an optimal interfacial behavior was observed for the P/K−BF-3 samples, which presented the highest storage modulus. When added in excess, APTES weakened interfacial adhesion (self-reaction leading to aggregated silanol crystals), which caused a significant fall in the properties at the given temperature range (P/K−BF-4 and P/K−BF-5). Overall, the results are consistent with those obtained from static mechanical tests.

The loss modulus of PBS-based biocomposites is shown in Fig. 7b. The peak of the loss modulus was assigned to the glass transition temperature (*Tg*) (Huda et al., 2008). Compared to the PBS-based biocomposites that used unmodified bamboo fibers, the *Tg* shifted to higher temperature in the case of those reinforced with K−BF and PDA-BF. This is due to the interfacial reinforcement, which increased the viscosity of the PBS matrix and restricted molecular motion (Wang et al., 2013). The greater interfacial enhancement was achieved *via* secondary amino silane grafting, leading to less dissipation of energy to overcome the internal friction, generated by the molecular motion, and resulted in a much higher *Tg* (P/K−BF-1, P/K−BF-2 and P/K−BF-3).

Compared to the BF-reinforced biocomposites, the values of tan δ of the biocomposites reinforced with K−BF and PDA-BF were significantly reduced, Fig. 7c. This effect might be ascribed to the enhanced interfacial adhesion between the bamboo fibers and PBS matrix, which contributed to a reduced macromolecular mobility. The minimum tan δ was obtained for P/K−BF-3 biocomposites, corresponding to the optimal static mechanical properties. The better interfacial adhesion between the bamboo fibers and the PBS matrix improved the stress transfer and load-bearing capacity, which hindered the inner molecular motion of the biocomposites.

3.7. Morphology of fractured biocomposites

The micrographs of the fractured area of PBS-based biocomposites are shown in Fig. 8. The poor interfacial adhesion between the unmodified bamboo fibers and PBS matrix caused abundant and irregularly distributed voids, generated by fiber pull-out, Fig. 8a. The surface modification via amino silane grafting and PDA surface treatment enhanced the interfacial adhesion between the fibers and the PBS matrix and thus facilitated stress transfer (Fig. 8b and c). The interfacial bonding between the bamboo fibers and the PBS matrix, as seen in the fractured surfaces, further improved with the combined PDA-silane surface treatment. As discussed in the case of the static mechanical properties, an appropriate APTES addition (P/K−BF-3) contributed to an optimum interfacial adhesion, which promoted a balanced stress transfer and avoided interfacial damage under load, thus creating an ideal binding between fibers and PBS (Fig. 8f). Fiber detachment from the PBS matrix occurred easily at low amino silane grafting (Fig. 8d and e). The aggregated silanol crystals produced by self-reaction generated an excess of amino silane grafting, causing stress concentration and producing a weak interfacial adhesion between the fibers and the PBS matrix (Fig. 8g and h).

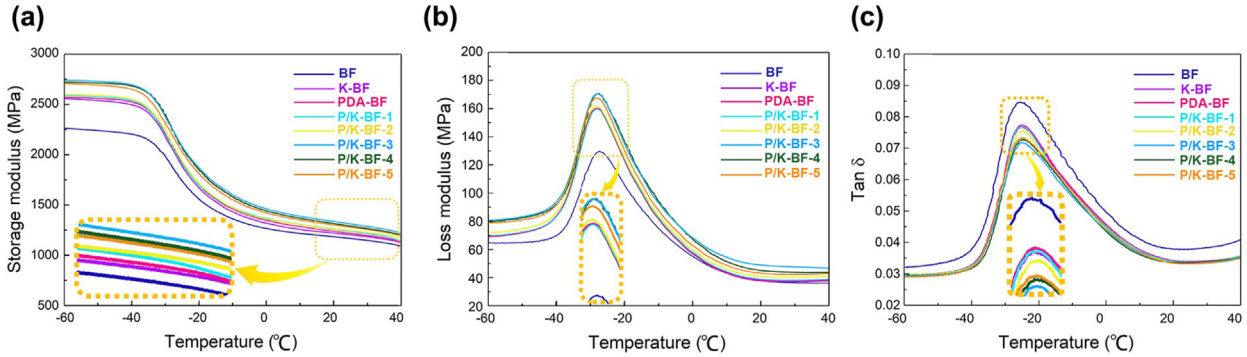

Fig. 7. DMA curves of PBS-based biocomposites: **(a)** storage modulus; **(b)** loss modulus; and **(c)** loss factor (tan δ).

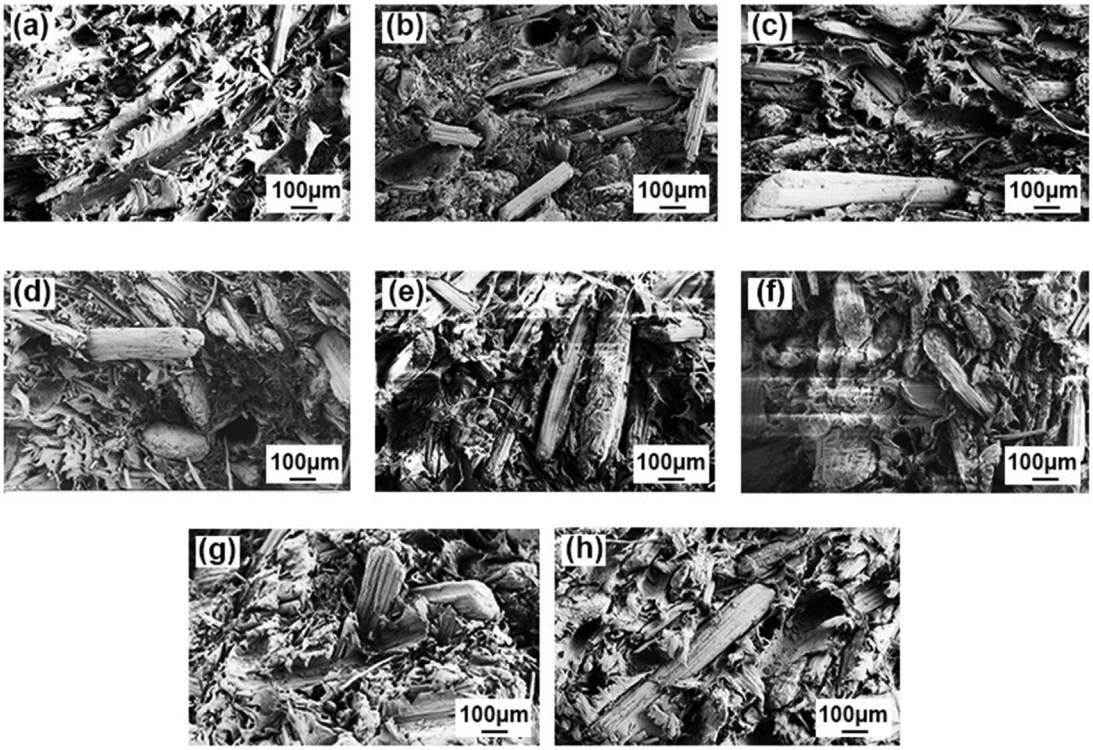

Fig. 8. SEM images of the fractured areas of **(a)** BF; **(b)** K–BF; **(c)** PDA-BF; **(d)** P/K–BF-1; **(e)** P/K–BF-2; **(f)** P/K–BF-3; **(g)** P/K–BF-4; and **(h)** P/K–BF-5.

3.8. Interfacial adhesion mechanism

The interfacial adhesion of bamboo fiber-reinforced PBS biocomposites is schematically illustrated in Fig. 9. The hybrid PDA-based coating was coupled onto the fiber surface by a simple oxidation self-polymerization of dopamine and secondary grafting of amino silane via Michael addition and/or Schiff-based reactions. This procedure introduced the crosslinked PDA-silanol system on the surface of the bamboo fibers, which formed a network with the PBS chains, leading to the improvement of interfacial adhesion. Meanwhile, as discussed in the case of the morphology of bamboo fibers, the highly increased fiber surface roughness generated from the crosslinked PDA-silanol network led to a tougher interfacial interlocking between the fibers and the PBS matrix, resulting in an enhanced interfacial adhesion in the PBS-based biocomposites. Besides, the tight adhesion of fibers and PBS matrix allowed for the uniform transfer of stress from the matrix to the fibers to restrict the chain mobility under external load. To better elucidate the interfacial bonding in the biocomposites, the movement and bonding behavior of the main molecules (cellulose, PDA, PDA-silanol complex, and PBS) were simulated at the molecular level (Fig. S4). As expected, the lowest interaction energy was found between PDA-silanol complex and PBS molecules with value of 197 kJ/mol, indicating that a more stable system was established by using fibers decorated with PDA-silanol and acting as the reinforcing phase in the PBS matrix. The enhancement mechanism could be attributed to the promotion of van der Waals forces and hydrogen bonding interaction between BF/PBS biocomposite after the introduction of PDA-silanol complex network at the interface. To sum up, these results further revealed a strong interfacial adhesion between the modified BF and the PBS matrix.

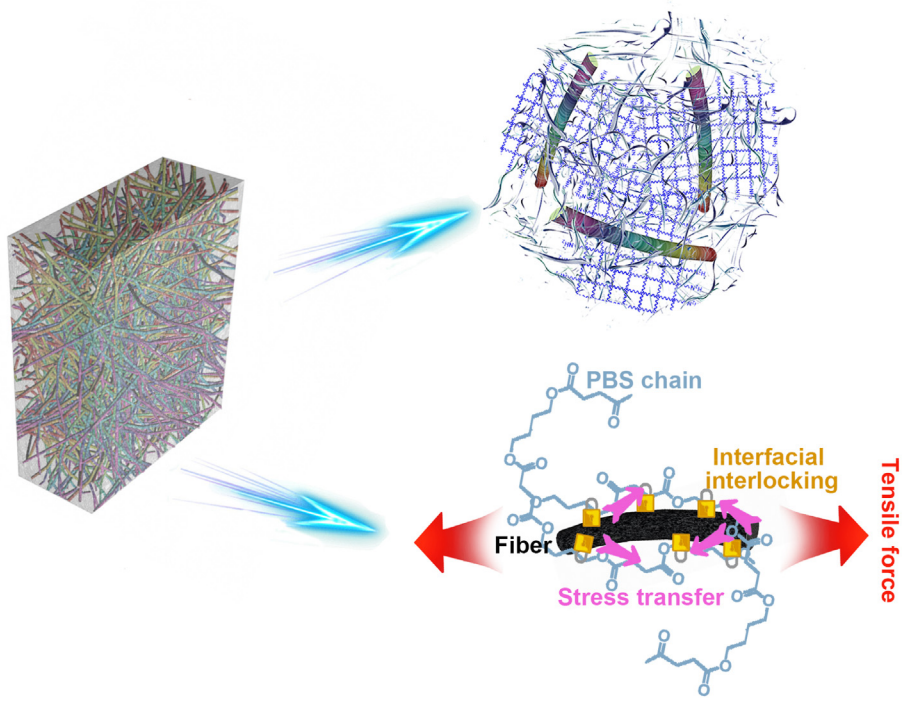

Fig. 9. The proposed mechanism leading to the interfacial adhesion between PBS and PDA-silanol treated bamboo fibers.

3.9. Hygroscopicity

The equilibrium moisture content of PBS-based biocomposites is shown in Fig. 10a and b (adsorption and desorption isotherms). The equilibrium moisture content of all the PBS-based biocomposites increased with the increased environmental humidity. The change of the equilibrium moisture content upon desorption also showed the same trends. The values of equilibrium moisture during absorption were lower than those during desorption, which is typical of other cellulosic materials such as solid wood, oriented strand board and medium density fiberboard (Jamaludin et al., 2013; Ji et al., 2017; Jonoobi et al., 2018; Van Houts et al., 2004; Wang and Morrell, 2004). Principally, PBS-based biocomposites presented water diffusion pathways, in the interspaces and microcracks between the fibers and the PBS matrix (Liu et al., 2015), which are closely related to the interfacial adhesion of PBS-based biocomposites.

As was discussed in the context of the fracture morphology, the bonding between the bamboo fibers and the PBS matrix improved with the interfacial adhesion produced with amino silane grafting and PDA surface coupling. The reduced interspaces and microcracks of biocomposites reinforced with K–BF and PDA-BF resulted in a lower moisture absorption and desorption. The values of the moisture absorption and desorption reached a minimum at the optimum APTES addition (P/K–BF-3), which contributed to a strong interfacial adhesion and restricted water movement in the PBS-based biocomposites. The samples with low (P/K–BF-1 and P/K–BF-2) or excess (P/K–BF-4 and P/K–BF-5) APTES loading did not lead to tight interfaces and were less effective in preventing moisture transport (absorption/desorption).

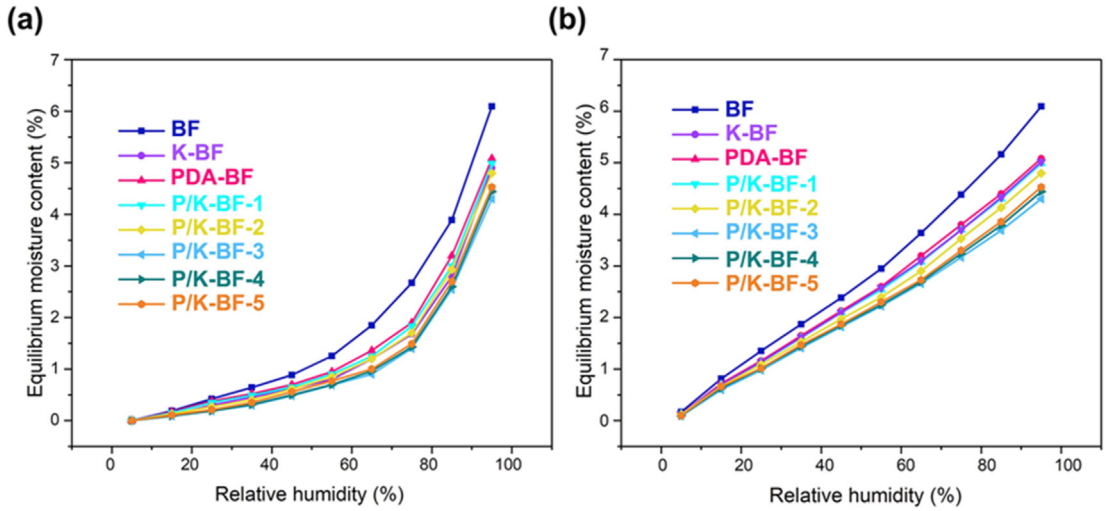

Fig. 10. The equilibrium moisture content: **(a)** absorption; and **(b)** desorption isotherms of PBS-based biocomposites.

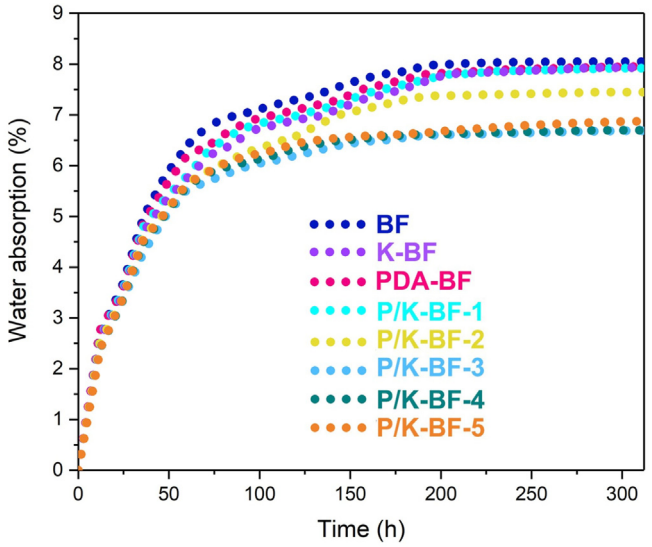

Fig. 11. Water absorption isotherms of PBS-based biocomposites.

3.10. Water absorption

The water absorption profiles for the various PBS-based biocomposites and the corresponding final equilibrium moisture are given in Fig. 11. The water absorbed by all PBS-based biocomposites showed a rapid initial increase (first 100 h), followed by slower dynamics. Finally, a saturation level was reached, after which no further absorption took place. In general, the hydrophobic character of PBS limited water absorption, to about 1% (Lee et al., 2013). The hydrophilic nature of the bamboo fibers and the interfacial adhesion were leading factors affecting water absorption. The biocomposites reinforced by unmodified bamboo fibers presented the highest water absorption, which is the result of the poor interfacial adhesion between the fibers and the PBS matrix, which generated abundant gaps and exposed the hydrophilic bamboo fibers. Conversely, an enhanced adhesion resulted in a tighter coverage of the fibers within PBS matrix, reducing the void spaces. This resulted in a hindered water absorption and low equilibrium moisture content. The optimal interfacial adhesion of P/K−BF-3 created a strong barrier for water diffusion, which led to a minimum equilibrium moisture content (the moisture content was reduced from 8% to 6.6%).

4. Conclusion

In summary, a facile and efficient approach to develop strong interfacial interactions between PBS and bamboo fibers is presented. The process involves reactive PDA coupling with the surface of bamboo fibers via self-polymerization of dopamine. Hydrolyzed amino silanol generated from APTES bonded covalently to PDA through functional catechol via Michael addition and/or Schiff base reactions. The fiber-reinforced PBS biocomposites were fabricated through a simple hot pressing procedure. The crosslinked PDA-silanol network formed on the surface of the bamboo fibers promoted interfacial adhesion with the PBS matrix. The improvement in the mechanical performance of the as-prepared biocomposites surpasses most of the natural fiber−reinforced polymer composites. Meanwhile, a lower hygroscopicity and higher water resistance were achieved due to the enhanced interfacial adhesion between the treated fibers and the PBS matrix. This work guides the future exploration on developing high-performance natural fiber-reinforced polymer composites.

CRediT authorship contribution statement

Gonghua Hong: Conceptualization, Methodology, Validation, Formal analysis, Software, Investigation, Data curation, Writing − original draft, Writing − review & editing. **Haitao Cheng:** Methodology. **Shuangbao Zhang:** Supervision, Project administration, Funding acquisition. **Orlando J. Rojas:** Supervision, Conceptualization, Writing − review & editing, Validation, Project administration.

Declaration of competing interest

The authors declare that they have no known competing financial interests or personal relationships that could have appeared to influence the work reported in this paper.

Acknowledgement

The financial support for this work was provided by the National Natural Science Foundation of China (31670571) and Beijing Natural Science Foundation (6202024). Orlando J. Rojas and Gonghua Hong acknowledge funding from the European Research Council under the European Union's Horizon 2020 research and innovation program (ERC Advanced Grant Agreement No. 788489, "BioElCell"). Orlando J. Rojas is grateful to the Canada Excellence Research Chair initiative and the Canada Foundation for Innovation (CFI). Gonghua Hong is grateful to the funding from China Scholarship Council.

Appendix A. Supplementary data

Supplementary data to this article can be found online at https://doi.org/10.1016/j.jclepro.2021.126587.

References

Akubueze, E.U., Ezeanyanaso, C.S., Muniru, S.O., Igwe, C.C., Nwauzor, G.O., Ugoh, U., Nwaze, I.O., Mafe, O., Nwaeche, F.C., 2019. Reinforcement of plaster of paris (POP) for suspended ceilings applications using kenaf bast fibre. Curr. J. Appl. Sci. Tech. 36 (6), 1−6.

Chen, F., Han, G.P., Li, Q.D., Gao, X., Cheng, W.L., 2017. High-temperature hot air/silane coupling modification of wood fiber and its effect on properties of wood fiber/HDPE composites. Materials 10 (3).

Chen, Q., Bai, W., Xu, Y., Lin, J., 2012. Chemical structure and reaction scheme of modified bamboo powder with silane coupling agent. Chem. Ind. For. Prod. 32 (6), 27−31.

Claramunt, J., Fernandez-Carrasco, L.J., Ventura, H., Ardanuy, M., 2016. Natural fiber nonwoven reinforced cement composites as sustainable materials for building envelopes. Construct. Build. Mater. 115, 230−239.

Dahy, H., 2019. Natural fibre-reinforced polymer composites (NFRP) fabricated from lignocellulosic fibres for future sustainable architectural applications, case studies: segmented-shell construction, acoustic panels, and furniture. Sensors 19 (3).

Fang, L., Chang, L., Guo, W.J., Chen, Y.P., Wang, Z., 2014. Influence of silane surface modification of veneer on interfacial adhesion of wood-plastic plywood. Appl. Surf. Sci. 288, 682−689.

Faruk, O., Bledzki, A.K., Fink, H.P., Sain, M., 2014. Progress report on natural fiber reinforced composites. Macromol. Mater. Eng. 299 (1), 9−26.

Fazita, M.R.N., Jayaraman, K., Bhattacharyya, D., Haafiz, M.K.M., Saurabh, C.K., Hussin, M.H., Khalil, H.P.S.A., 2016. Green composites made of bamboo fabric and poly (lactic) acid for packaging applications-A review. Materials 9 (6).

Feng, J.R., Fan, H.L., Zha, D.A., Wang, L., Jin, Z.X., 2016. Characterizations of the formation of polydopamine-coated halloysite nanotubes in various pH environments. Langmuir 32 (40), 10377−10386.

Ferreira, S.R., Pepe, M., Martinelli, E., Silva, F.D., Toledo, R.D., 2018. Influence of natural fibers characteristics on the interface mechanics with cement based matrices. Compos. B Eng. 140, 183−196.

Gao, R.N., Xiao, S.L., Gan, W.T., Liu, Q., Amer, H., Rosenau, T., Li, J., Lu, Y., 2018. Mussel adhesive-inspired design of superhydrophobic nanofibrillated cellulose aerogels for oil/water separation. Acs Sustain. Chem. Eng. 6 (7), 9047−9055.

Gao, X., Li, Q.D., Cheng, W.L., Han, G.P., Xuan, L.H., 2016. Optimization of high temperature and pressurized steam modified wood fibers for high-density polyethylene matrix composites using the orthogonal design method. Materials 9 (10).

Gigli, M., Fabbri, M., Lotti, N., Gamberini, R., Rimini, B., Munari, A., 2016.

Poly(butylene succinate)-based polyesters for biomedical applications: a review. Eur. Polym. J. 75, 431–460.
Gopinath, R., Poopathi, R., Saravanakumar, S.S., 2019. Characterization and structural performance of hybrid fiber-reinforced composite deck panels. Adv. Compos. Hybrid Mater. 2 (1), 115–124.
Gu, C.W., Huang, X.C., Shi, M.W., Zhang, M., Wang, X.L., Zheng, Z., 2013. Bio-inspired layer-by-layer assembled hybrid films for improvement of mechanical properties. Polym. Compos. 34 (8), 1261–1268.
Hao, M.Z., Tang, M.M., Wang, W.C., Tian, M., Zhang, L.Q., Lu, Y.L., 2016. Silver-nanoparticle-decorated multiwalled carbon nanotubes prepared by poly(dopamine) functionalization and ultraviolet irradiation. Compos. B Eng. 95, 395–403.
Huang, Z.L., Qian, L.W., Yin, Q.J., Yu, N., Liu, T.G., Tian, D., 2018. Biodegradability studies of poly(butylene succinate) composites filled with sugarcane rind fiber. Polym. Test. 66, 319–326.
Huda, M.S., Drzal, L.T., Mohanty, A.K., Misra, M., 2008. Effect of fiber surface-treatments on the properties of laminated biocomposites from poly(lactic acid) (PLA) and kenaf fibers. Compos. Sci. Technol. 68 (2), 424–432.
Huo, Z.Y., Liu, H., Yu, C., Wu, Y.H., Hu, H.Y., Xie, X., 2019. Elevating the stability of nanowire electrodes by thin polydopamine coating for low-voltage electroporation-disinfection of pathogens in water. Chem. Eng. J. 369, 1005–1013.
Hwang, S.H., Kang, D., Ruoff, R.S., Shin, H.S., Park, Y.B., 2014. Poly(vinyl alcohol) reinforced and toughened with poly(dopamine)-treated graphene oxide, and its use for humidity sensing. ACS Nano 8 (7), 6739–6747.
Iwata, T., 2015. Biodegradable and bio-based polymers: future prospects of eco-friendly plastics. Angew. Chem. Int. Ed. 54 (11), 3210–3215.
Jamaludin, M.A., Taib, M.N.A.M., Zakaria, M.N., Abu Kassim, M., Zainuddin, N.S., 2013. Non-steady state moisture diffusion flow in homogenous pineapple leaves particleboard. Adv. Mater. Res. 774–776, 279–283.
Ji, X.D., Li, B., Yuan, B.N., Guo, M.G., 2017. Preparation and characterizations of a chitosan-based medium-density fiberboard adhesive with high bonding strength and water resistance. Carbohydr. Polym. 176, 273–280.
Jonoobi, M., Ghorbani, M., Azarhazin, A., Hosseinabadi, H.Z., 2018. Effect of surface modification of fibers on the medium density fiberboard properties. Eur. J. Wood Wood Prod. 76 (2), 517–524.
Khalil, H.P.S.A., Bhat, A.H., Yusra, A.F.I., 2012. Green composites from sustainable cellulose nanofibrils: a review. Carbohydr. Polym. 87 (2), 963–979.
Kohan, L., Martins, C.R., Duarte, L.O., Pinheiro, L., Baruque-Ramos, J., 2019. Panorama of natural fibers applied in Brazilian footwear: materials and market. Sn Appl. Sci. 1 (8).
Lee, B.P., Messersmith, P.B., Israelachvili, J.N., Waite, J.H., 2011. Mussel-inspired adhesives and coatings. Annu. Rev. Mater. Res. 41, 99–132.
Lee, H., Dellatore, S.M., Miller, W.M., Messersmith, P.B., 2007. Mussel-inspired surface chemistry for multifunctional coatings. Science 318 (5849), 426–430.
Lee, J.M., Ishak, Z.A.M., Taib, R.M., Law, T.T., Thirmizir, M.Z.A., 2013. Mechanical, thermal and water absorption properties of kenaf-fiber-based polypropylene and poly(butylene succinate) composites. J. Polym. Environ. 21 (1), 293–302.
Lee, S.J., Lee, D., Yoon, T.R., Kim, H.K., Jo, H.H., Park, J.S., Lee, J.H., Kim, W.D., Kwon, I.K., Park, S.A., 2016. Surface modification of 3D-printed porous scaffolds via mussel-inspired polydopamine and effective immobilization of rhBMP-2 to promote osteogenic differentiation for bone tissue engineering. Acta Biomater. 40, 182–191.
Lee, S.M., Cho, D., Park, W.H., Lee, S.G., Han, S.O., Drzal, L.T., 2005. Novel silk/poly(butylene succinate) biocomposites: the effect of short fibre content on their mechanical and thermal properties. Compos. Sci. Technol. 65 (3–4), 647–657.
Levy, M.J., Matharu, M.S., Goadsby, P.J., 2003. Prolactinomas, dopamine agonists and headache: two case reports. Eur. J. Neurol. 10 (2), 169–173.
Liu, D.G., Song, J.W., Anderson, D.P., Chang, P.R., Hua, Y., 2012. Bamboo fiber and its reinforced composites: structure and properties. Cellulose 19 (5), 1449–1480.
Liu, F.H., Han, G.P., Cheng, W.L., Wu, Q.L., 2015. Sorption isotherm of southern yellow pine-high density polyethylene composites. Materials 8 (1), 368–378.
Liu, W.D., Xie, T.S., Qiu, R.H., 2016. Bamboo fibers grafted with a soybean-oil-based monomer for its unsaturated polyester composites. Cellulose 23 (4), 2501–2513.
Lu, Z.S., Xiao, J., Wang, Y., Meng, M., 2015. In situ synthesis of silver nanoparticles uniformly distributed on polydopamine-coated silk fibers for antibacterial application. J. Colloid Interface Sci. 452, 8–14.
Majeed, K., Jawaid, M., Hassan, A., Abu Bakar, A., Khalil, H.P.S.A., Salema, A.A., Inuwa, I., 2013. Potential materials for food packaging from nanoclay/natural fibres filled hybrid composites. Mater. Des. 46, 391–410.
Meng, Y., Wang, M.J., Tang, M.F., Hong, G.H., Gao, J.M., Chen, Y., 2017. Preparation of robust superhydrophobic halloysite clay nanotubes via mussel-inspired surface modification. Appl. Sci. 7 (11).
Palanisamy, S., Thangavelu, K., Chen, S.M., Gnanaprakasam, P., Velusamy, V., Liu, X.H., 2016. Preparation of chitosan grafted graphite composite for sensitive detection of dopamine in biological samples. Carbohydr. Polym. 151, 401–407.
Palladino, P., Bettazzi, F., Scarano, S., 2019. Polydopamine: surface coating, molecular imprinting, and electrochemistry-successful applications and future perspectives in (bio)analysis. Anal. Bioanal. Chem. 411 (19), 4327–4338.
Peng, L., Zhou, S.L., Yang, B., Bao, M.M., Chen, G.J., Zhang, X.H., 2017. Chemically modified surface having a dual-structured hierarchical topography for controlled cell growth. Acs Appl. Mater. Inter. 9 (28), 24339–24347.
Perez-Fonseca, A.A., Robledo-Ortiz, J.R., Moscoso-Sanchez, F.J., Fuentes-Talavera, F.J., Rodrigue, D., Gonzalez-Nunez, R., 2015. Self-hybridization and coupling agent effect on the properties of natural fiber/HDPE composites. J. Polym. Environ. 23 (1), 126–136.
Salarizadeh, P., Javanbakht, M., Pourmandian, S., Beydaghi, H., 2016. Influence of amine-functionalized iron titanate as filler for improving conductivity and electrochemical properties of SPEEK nanocomposite membranes. Chem. Eng. J. 299, 320–331.
Scarponi, C., Messano, M., 2015. Comparative evaluation between E-Glass and hemp fiber composites application in rotorcraft interiors. Compos. B Eng. 69, 542–549.
Shukla, S.K., Lavon, A., Shmulevich, O., Ben-Yoav, H., 2018. The effect of loading carbon nanotubes onto chitosan films on electrochemical dopamine sensing in the presence of biological interference. Talanta 181, 57–64.
Song, Y.Y., Jiang, H.J., Wang, B.B., Kong, Y., Chen, J., 2018. Silver-incorporated mussel-inspired polydopamine coatings on mesoporous silica as an efficient nano-catalyst and antimicrobial agent. Acs Appl. Mater. Inter. 10 (2), 1792–1801.
Takatani, M., Ito, H., Ohsugi, S., Kitayama, T., Saegusa, M., Kawai, S., Okamoto, T., 2000. Effect of lignocellulosic materials on the properties of thermoplastic polymer/wood composites. Holzforschung 54 (2), 197–200.
Tang, C.M., Tian, Y.H., Hsu, S.H., 2015. Poly(vinyl alcohol) nanocomposites reinforced with bamboo charcoal nanoparticles: mineralization behavior and characterization. Materials 8 (8), 4895–4911.
Tang, J.T., Song, Y., Zhao, F.P., Spinney, S., Bernardes, J.D., Tam, K.C., 2019. Compressible cellulose nanofibril (CNF) based aerogels produced via a bio-inspired strategy for heavy metal ion and dye removal. Carbohydr. Polym. 208, 404–412.
Tavares, T.D., Antunes, J.C., Ferreira, F., Felgueiras, H.P., 2020. Biofunctionalization of natural fiber-reinforced biocomposites for biomedical applications. Biomolecules 10 (1).
Vaisanen, T., Das, O., Tomppo, L., 2017. A review on new bio-based constituents for natural fiber-polymer composites. J. Clean. Prod. 149, 582–596.
Van Houts, J.H., Wang, S.Q., Shi, H.P., Pan, H.J., Kabalka, G.W., 2004. Moisture movement and thickness swelling in oriented strandboard, part 1. Analysis using nuclear magnetic resonance microimaging. Wood Sci. Technol. 38 (8), 617–628.
Wang, L., Shi, Y.X., Chen, S.X., Wang, W.C., Tian, M., Ning, N.Y., Zhang, L.Q., 2017. Highly efficient mussel-like inspired modification of aramid fibers by UV-accelerated catechol/polyamine deposition followed chemical grafting for high-performance polymer composites. Chem. Eng. J. 314, 583–593.
Wang, W., Zhang, G.X., Zhang, W.Z., Guo, W.H., Wang, J.K., 2013. Processing and thermal behaviors of poly (butylene succinate) blends with highly-filled starch and glycerol. J. Polym. Environ. 21 (1), 46–53.
Wang, W.H., Morrell, J.J., 2004. Water sorption characteristics of two wood-plastic composites. For. Prod. J. 54 (12), 209–212.
Wei, L.Q., McDonald, A.G., Freitag, C., Morrell, J.J., 2013. Effects of wood fiber esterification on properties, weatherability and biodurability of wood plastic composites. Polym. Degrad. Stabil. 98 (7), 1348–1361.
Wu, F.C., Pu, N., Ye, G., Sun, T.X., Wang, Z., Song, Y., Wang, W.Q., Huo, X.M., Lu, Y.X., Chen, J., 2017. Performance and mechanism of uranium adsorption from seawater to poly(dopamine)-inspired sorbents. Environ. Sci. Technol. 51 (8), 4606–4614.
Wu, Q., Shao, Q., Li, Q., Duan, Q., Li, Y.H., Wang, H.G., 2018. Dual carbon-confined SnO2 hollow nanospheres enabling high performance for the reversible storage of alkali metal ions. Acs Appl. Mater. Inter. 10 (18), 15642–15651.
Wu, W.H., Yang, L.T., Zhao, F.Q., Zeng, B.Z., 2017. A vanillin electrochemical sensor based on molecularly imprinted poly(1-vinyl-3-octylimidazole hexafluoride phosphorus) -multi-walled carbon nanotubes@polydopamine-carboxyl single-walled carbon nanotubes composite. Sensor. Actuator. B Chem. 239, 481–487.
Xia, C.L., Yu, J., Shi, S.Q., Qiu, Y., Cai, L.P., Wu, H.F., Ren, H., Nie, X., Zhang, H.L., 2017. Natural fiber and aluminum sheet hybrid composites for high electromagnetic interference shielding performance. Compos. B Eng. 114, 121–127.
Xie, Y.J., Hill, C.A.S., Xiao, Z.F., Militz, H., Mai, C., 2010. Silane coupling agents used for natural fiber/polymer composites: a review. Compos. Part A-Appl. S. 41 (7), 806–819.
Xiong, S.Q., Wang, Y., Yu, J.R., Chen, L., Zhu, J., Hu, Z.M., 2014. Polydopamine particles for next-generation multifunctional biocomposites. J. Mater. Chem. 2 (20), 7578–7587.
Xu, C.H., Shamey, R., Hinks, D., 2010a. Activated peroxide bleaching of regenerated bamboo fiber using a butyrolactam-based cationic bleach activator. Cellulose 17 (2), 339–347.
Xu, G.Q., Wang, L.H., Liu, J.L., Wu, J.Z., 2013. FTIR and XPS analysis of the changes in bamboo chemical structure decayed by white-rot and brown-rot fungi. Appl. Surf. Sci. 280, 799–805.
Xu, Q., Cui, Y.H., Wang, X.X., Xia, Z.Z., Han, C., Wang, J.B., 2010b. Moisture absorption properties of wood-fiber-reinforced recycled polypropylene matrix composites. J. Vinyl Addit. Technol. 16 (1), 50–57.
Yang, Z.Z., Feng, X.H., Xu, M., Rodrigue, D., 2020. Properties of poplar fiber/PLA composites: comparison on the effect of maleic anhydride and KH550 modification of poplar fiber. Polymers 12 (3).
Yao, L.H., Wang, Y.J., Li, Y., Duan, J.K., 2017. Thermal properties and crystallization behaviors of polylactide/redwood flour or bamboo fiber composites. Iran. Polym. J. (Engl. Ed.) 26 (2), 161–168.
Yuan, J.Y., Zhang, Z.Z., Yang, M.M., Guo, F., Men, X.H., Liu, W.M., 2017. Surface modification of hybrid-fabric composites with amino silane and polydopamine for enhanced mechanical and tribological behaviors. Tribol. Int. 107, 10–17.
Yusup, E.M., Mahzan, S., Kamaruddin, M.A.H., 2019. Natural fiber reinforced polymer for the application of sports equipment using mold casting method. Int.

Conf. Mech. Eng. Res. Appl. 494.
Zhan, Y.Q., Zhang, J.M., Wan, X.Y., Long, Z.H., He, S.J., He, Y., 2018. Epoxy composites coating with Fe3O4 decorated graphene oxide: modified bio-inspired surface chemistry, synergistic effect and improved anti-corrosion performance. Appl. Surf. Sci. 436, 756–767.
Zhang, H., Bre, L.P., Zhao, T.Y., Zheng, Y., Newland, B., Wang, W.X., 2014. Mussel-inspired hyperbranched poly(amino ester) polymer as strong wet tissue adhesive. Biomaterials 35 (2), 711–719.
Zhang, X.P., Wang, F., Keer, L.M., 2015. Influence of surface modification on the microstructure and thermo-mechanical properties of bamboo fibers. Materials 8 (10), 6597–6608.
Zhao, J., Li, C.L., Liu, R., 2018. Enhanced oxygen reduction of multi-Fe3O4@carbon core-shell electrocatalysts through a nanoparticle/polymer co-assembly strategy. Nanoscale 10 (13), 5882–5887.
Zhou, M., Li, Y.H., He, C., Jin, T.X., Wang, K., Fu, Q., 2014. Interfacial crystallization enhanced interfacial interaction of Poly (butylene succinate)/ramie fiber biocomposites using dopamine as a modifier. Compos. Sci. Technol. 91, 22–29.